An Online Trajectory Generator-Based Impedance Control For Co-manipulation Tasks

Sarra Jlassi, Sami Tliba, Yacine Chitour

An Online Trajectory Generator-Based Impedance Control For Co-manipulation Tasks

Authors: *Sarra Jlassi, Sami Tliba and Yacine Chitour*

S. Jlassi, S. Tliba and Y. Chitour are with Laboratoire des Signaux et Systèmes UMR8506, Univ Paris-Sud, CNRS, SUPELEC, 3 rue Joliot Curie, 91192 Gif-sur-Yvette, France (corresponding author e-mail: sami.tliba@lss.supelec.fr).

Université Paris-Sud XI,
U.F.R. des Sciences d'Orsay
Layout by Sami TLIBA, © September 2013

UMR : Laboratoire des Signaux & Systèmes
Projet : Robotic comanipulation
Type : Preprint to "2014 IEEE HAPTICS Symposium"

Abstract

During human robot interaction (HRI), the resulting cooperative motion should be truly intuitive and should not restrict in any way the operator's willingness to move the robot such he would like. The idea proposed in this paper consists in considering the HRI problem for handling tasks as a constrained optimal control problem. For this purpose, we have designed a new modified impedance control method named *Online Trajectory-Based Impedance (OTBI) Control*. This method relies on the implementation of a specific event controlled online trajectory generator (OTG) associated to a classical structure of impedance control allowing a very good tracking of the generated trajectory. This OTG is designed so as to translate the human operator intentions to ideal trajectories that the robot must follow. It works as an automaton with two states of motion whose transitions are controlled by comparing the magnitude of the force to an adjustable threshold, in order to enable the operator to keep authority over the robot's states of motion. The key idea of this approach consists in generating a velocity trajectory for the end-effector that would stay collinear at every moment to the HRI force. The overall strategy is applied to a 2DOF robot.

keywords: Human-robot interaction, online trajectory generation, impedance control.

1 Introduction

For the past ten years, robots are more and more envisioned as helpers of mankind, closely cooperating with and assisting people in their daily life. Several active areas of research concern robots interacting physically with a human operator (HO). In (Charnnarong et al., 1995), robots help in alleviating therapists of the physical rigors of their work, freeing them to concentrate on patient needs. Robots excel at repetition and do not tire, so they can allow a patient to complete a greater number of moves in a therapy session, with improved consistency. Works of Kazerooni and Guo (1993) investigated techniques called extender or power assist, they are intended to boost the force capacity of human limbs while retaining the human brain as the high-level controller. These devices allow human operator and robot to exchange mutually informations: the HO applies small forces along a desired direction where he wants to drive the robot, and the robot's position is sensed by the HO. The robot assists the human during his motion while relieving him from the important effort without any human perceptible resistive forces like inertia, friction *etc*. Humans are skilled at complex tasks and are able to react very flexibly to unknown situations. Industrial robots are very strong, fast, persevering and accurate. It is important to note the difference between the frequencies with which a human operator and the robot can perform their tasks. Studies of Miyhoshi and Murata (2000) have shown that a human can perform a task with a frequency of up to 6Hz, which is much slower than the typical sampling frequency used in a robotic control scheme. During physical human-robot interaction (PHRI), the skills of both should be combined and the resulting cooperative motion should be truly intuitive and should not restrict in any way the human motion. This is often referred to as transparency. There are still many challenges on the road to achieving an efficient physical HRI (Santis et al., 2008). These challenges are mainly related to the fundamental problem of ensuring safety (stability) to the user and robot. Any collision involving the robot and the human must result in a soft bouncing of the robot. This is named compliant behavior. One of the most commonly used control approach to give interactive robots a compliant behavior is the so called impedance/admittance control (Akella et al., 1999; Lamy et al., 2010). Its purpose is to reduce the mechanical interaction point (IP) impedance so as to make it equal to that of HO (Buerger, 2005). In the context of co-manipulation for handling tasks, impedance control based methods have few drawbacks, particularly noticeable during the starting and the stopping phases. This paper presents a novel modified impedance control method named *Online Trajectory-Based Impedance (OTBI) Control*. This control method consists of an event controlled online trajectory generator associated to a classical structure of impedance control allowing a very good tracking of the generated trajectory. It is obvious that the force applied by the HO is the only physically exchanged signal, showing the robot how to move according to his willingness. Indeed, this force gives the information about the desired displacement direction of the end-effector. But, this direction should necessarily be collinear to the IP velocity. In (Jlassi et al., 2012), the idea of maintaining to the maximum the collinearity of the end-effector velocity and the interaction force was proposed to concur in achieving a transparent co-manipulation. The required force to accomplish the co-manipulation

task is supplied by the robot's actuators, controlled in order to ensure a good trajectory tracking. Furthermore, for sake of safety, we consider that the displacement velocity should not entirely depend on HO's desire but must be conform to a given velocity template. The literature provides a very rich set of approaches and algorithms of trajectory generation for industrial manipulators (Kroger, 2012).

In this paper we address the case of force sensor-based trajectory generation. The interaction force processing should contribute to both interpreting the triggering times of movements/immobility and in commanding how the robot has to move or stop, while leaving the final position under the human authority. The trajectory is calculated on-line, i.e. each desired position is updated during every control cycle because the input values based on the HO force (intensity and direction) may change unpredictably.

The remainder of this paper is organized as follows: After a brief study in Section 2 about the impedance control evolution, an analysis of the co-manipulation requirements and their consequences on the problem statement is presented in Section 3. The control strategy based on the criterion of collinearity between the interaction force and the end-effector velocity is presented in Section 4. The description of the proposed OTG is developed in Subsection 4.3. The controller design is explained in Section 4.4. Section 5 proposes an illustration of this approach for a 2DOF robot.

2 Impedance control for physical human robot interaction

Based on studies analyzing the cooperation between two human operators when accomplishing a heavy loads handling task, Ikeura and Inooka (1995) have investigated the HO characteristics and have shown that the damping parameters in the impedance model are the predominant coefficients that allow setting the acceleration/deceleration features in the context of PHRI. They demonstrated experimentally that the effects of stiffness and inertia parameters are negligible. In the context of human-robot co-manipulation for handling tasks classical impedance control based methods have shown few drawbacks, particularly noticeable during the starting and the stopping phases. First, as explained in (Duchaine and Gosselin, 2009), the use of a fixed virtual damping can lead to an inefficient co-manipulation. Indeed, if the damping is set to a low value the robot will tend to accelerate,then, when the HO wants to stop the robot the system will be unstable and the robot arm could collapse, which may cause a serious danger to the HO. In the case of high damping, the robot will be hard to manipulate and thereby restricts the human motion. In this latter case, the human operator can not operate as fast as if it is in cooperation with another HO. Another drawback of admittance control is related to security. Admittance control is known to potentially exhibit unstable behaviour when facing rigid environments (Surdilovic, 1996). This problem is difficult to be solved in the context of PHRI since human operators, who act as the environment, have a variable stiffness. In order to solve these problems, the so called variable impedance control was introduced. Several works dealing with this control method were published. Ikeura and Inooka (1995) proposed a variable impedance control where the virtual damping coefficient is chosen between two prescribed values according to the end-effector velocity. Later, in (Ikeura et al., 2002), they proposed to adjust on-line the damping parameters, in an optimal manner by minimizing a selected cost function. Tsumugiwa et al. (2002) have proposed an online adjustment of this coefficient based on a real-time estimation of the human arm stiffness. More recently, in order to insure a better PHRI with respect to transparency, it was proposed in (Duchaine and Gosselin, 2009) to continuously adapt the virtual damping coefficient as a function of the human *intention*. This method allows satisfying a good co-manipulation task. However, one drawback of this approach is that the estimation of the HO intention was performed using the time derivative of the measured force and position, for which the measurement noises can cause problems with the numerical differentiation (dividing by zero, *etc*). Unlike works dealing with variable impedance control whose challenge consists in avoiding dividing by zero, the main purpose of our approach consists in insuring a good trajectory tracking in the transient phases. This control method is primarily intended to overcome the limitations described previously while meeting the co-manipulation's requirements in terms of assistance, transparency and security.

3 Problem description

3.1 Notations

Let n be the total number of the Degrees Of Freedom (DOFs) and $q \in \mathbb{R}^n$ the vectors of the generalized joints displacements. The well-known dynamical model of the robot is given by

$$M(q)\ddot{q} + C(q,\dot{q})\dot{q} + g(q) = \tau + \tau_h, \tag{1}$$

where $q \in \mathbb{R}^n$, $\dot{q} \in \mathbb{R}^n$ and $\ddot{q} \in \mathbb{R}^n$ are the vectors of the generalized joints displacements, the generalized joints velocities and the generalized joints accelerations respectively. The vector of applied motor torques is denoted by $\tau \in \mathbb{R}^n$.The vector of HRI torques is denoted by $\tau_h = J^T(q)\overrightarrow{F}_h$, where $\overrightarrow{F}_h$ is the interaction force and $J(q)$ is the manipulator Jacobian matrix. The terms $M(q) \in \mathbb{R}^{n\times n}$, $C(q,\dot{q})\dot{q} \in \mathbb{R}^n$ and $g(q) \in \mathbb{R}^n$ are employed to denote the inertia matrix (symmetric and positive definite), the vector containing the centrifugal and Coriolis forces and the vector of gravitational forces respectively.

The forward kinematics and general relationships between the joints coordinates and the operational space coordinates and force variables are given as

$$\begin{aligned} \overrightarrow{X} &= f(q), \quad \dot{\overrightarrow{X}} = J(q)\dot{q}, \\ \ddot{\overrightarrow{X}} &= J\ddot{q} + \dot{J}\dot{q}, \quad \tau = J^T(q)F, \end{aligned} \tag{2}$$

where $\overrightarrow{X} \in \mathbb{R}^n$ is the operational space coordinate vector.

3.2 Co-manipulation requirements and trade-off

This work focuses on heavy load handling tasks characterized by having motion with moderate velocities. A potential application field for the strategy proposed in this paper is the manufacturing industry such as construction industry and assembly where material handling requires considerable efforts. The main purpose is reducing these efforts, decreasing the consumed time and the costs of these activities. The mechanical links of the considered robots are all of revolute type. A load is linked to the last arm (end-effector), which is also the arm that interacts with the HO. A force sensor measures the interaction force and gives its corresponding coordinates along each direction in the end-effector frame. It is assumed that all the robot actuators are torque controlled and that the measures of position and velocity are all accessible. The human-robot co-manipulation problem is considered here as the achievement of a master-slave relationship, for which the HO decides when and where the robot moves. In other words, the HO contributes in the co-manipulation process by making a visual feedback loop of the current robot configuration with the desired one that he has in mind. This problem consists in guaranteeing the safety of the HO while manipulating the robot from its end-effector and driving it to the desired position without having to exert the required force to move the load, or even to perceive the resistive forces due to the robot dynamics such as its strong inertia, joints friction etc. Hence, this problem should be designed in a way that it satisfies the co-manipulation's requirements *i.e.*security, assistance and transparency as detailed in (Jlassi et al., 2012). The level of importance of each requirement depends on the expected purpose of co-manipulation. For the case of heavy load handling task, ensuring the maximum possible of transparency may cause a serious danger for the operator. Thus a trade-off between transparency and security appears necessary. Here, this trade-off will be in favor of security.

The main difference between the proposed approach and other works dealing with PHRI lies in the sought control objectives formulation. Our control objectives are based on the key concept that the velocity of the Interaction Point (IP) should remain collinear at every moment to the force exerted by the HO while being of moderate amplitude. The collinearity concurs to achieve part of the transparency requirement whereas a velocity of moderate amplitude allows to partly fulfill the security. Indeed, the standard developed by the International Organization for Standardization (ISO) ISO-10218 specifies the safety requirements for the integration of industrial robots in the context of HRI by imposing an

upper bound to the velocity of the end-effector, it must not exceed $0.25m/s$. Moon and Virk (2009) presented a study on the various existing standards. All these studies show that the robot velocity is the most important parameter to control. In order to comply with the security constraint, the velocity of the robot must be bounded during the co-manipulation task. The acceleration and jerk must also be bounded to insure comfort for the HO.

Notice that exerting a force is the only way for the HO to transmit the information that contains intrinsically the desired direction of displacement and this direction is given by the velocity vector at each instant. In consequence, the measured force should serve in generating a trajectory for the end-effector velocity that this latter has to track. Moreover, the trajectory to track must be generated online by an appropriate real-time processing of this information.To cope with safety requirement, the kinetic energy stored by the robot during the motion has to be limited by imposing either a profile or a template to the desired trajectory for the end-effector velocity. A template basically consists in imposing an upper bound on the magnitude of the end-effector velocity. But in our case, this also requires imposing an upper bound on its successive derivatives in order to filter the tremors introduced by the exerted force. On the other hand, the choice of a profile, which consists in using parameterized functions, is easier to implement in an OTG and allows to cope with the problem of tremors.

This latter approach will thus be adopted in the sequel. The assistance requirement will be satisfied once the trajectory generation and its tracking will be properly achieved.

4 Control Strategy

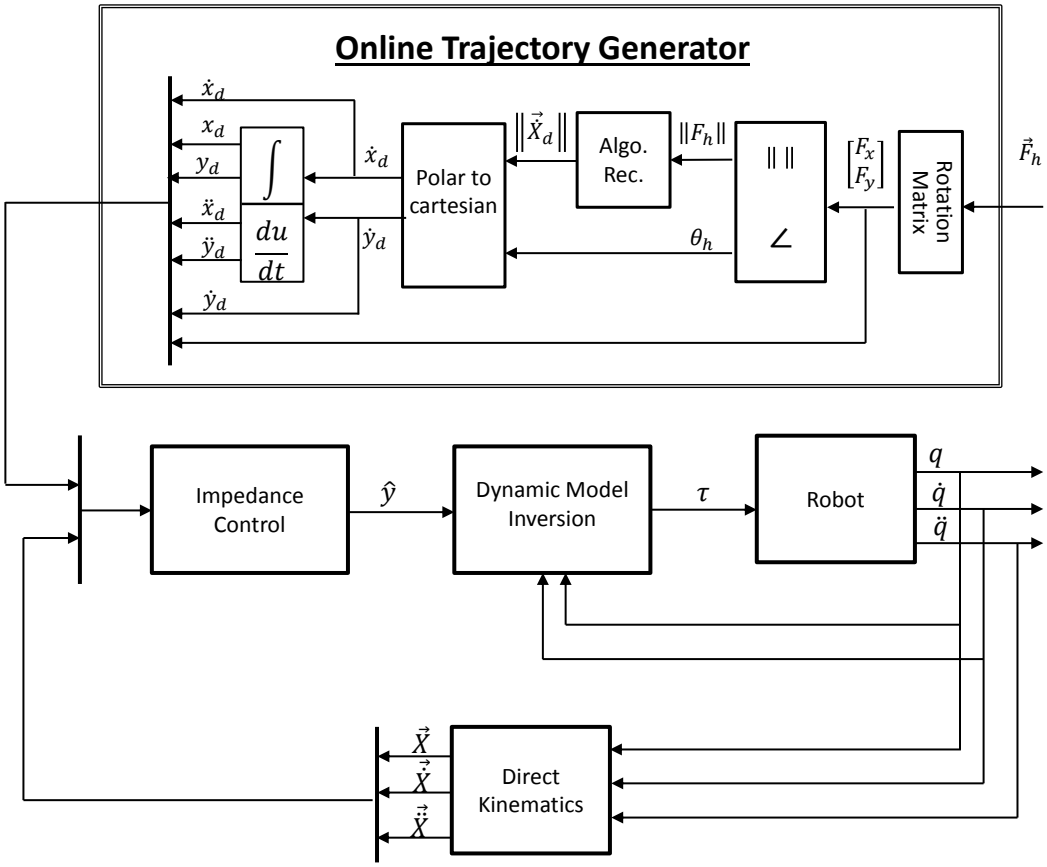

Figure 1: Control structure of planar robot.

As described previously, the control strategy should generate an appropriate trajectory to track for each DOF through an OTG-based impedance method. This method consists of an event controlled online trajectory generator component associated with a classical structure of impedance control as depicted in Figure 1, which allows to achieve a very good tracking of the generated trajectory.

4.1 Working frame and notations

In the following, we denote the desired task space positions, velocities, and accelerations as $\overrightarrow{X}_d$, $\dot{\overrightarrow{X}}_d$, and $\ddot{\overrightarrow{X}}_d$, respectively. Without loss of generality we will focus our development on the case of planar robots. Let $\overrightarrow{X} \in \mathbb{R}^2$ be the position vector of the end-effector and $\overrightarrow{F}_h \in \mathbb{R}^2$ the vector of forces exerted at the end-effector. This force vector is characterized by its Euclidean norm noted $F_h := \|\overrightarrow{F}_h\|$ and its orientation, defined by the unitary vector, noted $\overrightarrow{U}_{\theta_h}$ where θ_h is the angle formed by the interaction force $\overrightarrow{F}_h$ and a unitary vector of the fixed frame. Denote by $\overrightarrow{V}_{\theta_h}$ the unitary vector, orthogonal and positively oriented to $\overrightarrow{U}_{\theta_h}$.

4.2 Collinearity between force and end-effector velocity

As mentioned previously in Subsection (3.2), maintaining to the maximum the collinearity of the end-effector velocity and the interaction force while having the same direction, should concur in achieving a transparent co-manipulation. The co-manipulation expected requirements should lead the end-effector velocity and the interaction force to satisfy a relationship like

$$\dot{\overrightarrow{X}} = \chi\left(q, \dot{q}, \overrightarrow{F}_h\right), \tag{3}$$

under the constraints of zero cross-product

$$\dot{\overrightarrow{X}} \times \overrightarrow{F}_h = \overrightarrow{0} \tag{4}$$

and of positive scalar product

$$\left\langle \dot{\overrightarrow{X}} \,|\, \overrightarrow{F}_h \right\rangle > 0, \tag{5}$$

where $\chi(q, \dot{q}, F_h)$ is a mathematical operator that can be assimilated to an admittance relationship, but which expression is non-trivial and certainly hard to express analytically, because it has to satisfy all the requirements in an optimal manner. In particular, $\chi(q, \dot{q}, F_h)$ should be able to cope with discrete events such as the human decision of starting or stopping the robot motion, and to maintain a stable robot equilibrium position, robust to exogenous disturbances. Usually, this operator is described in frequency domain and taken as a linear admittance. As mentioned in Section 2, it is clear that a linear admittance cannot simply cope with start and stop phases.

In this paper, the seeking of the operator $\chi(q, \dot{q}, F_h)$ is addressed in a suboptimal way, through the use of the OTBI control, following the method described thereafter.

4.3 Online Trajectory Generator

a) Force intensity processing

Define two force thresholds, noted

- f_{th}: that allows distinguishing the intention to move the robot if the interaction force amplitude is greater than f_{th} and the willingness to stop it if the force is lower.

- f_{th-}: which is the hysteresis threshold defined to prevent small changes corresponding to unwanted triggering events, from having any effect.

Let h_r and h_f be the logical quantities defined as follows

- h_r switch to 1 when the force measurement crosses the threshold f_{th} with a rising edge,
- h_f switch to 1 when the force measurement crosses the threshold f_{th-} with a falling edge.

When h_r switch to 1, it means that the robot enters into a state of motion, noted Σ_{motion}, and it remains there. It is therefore an event from which two phases follow each other, a transient phase corresponding to the motion startup, noted ϕ_{rise}, and a phase of established motion, ϕ_{cruise}. When h_f switch to 1, it means that the robot enters into a state of immobility, noted Σ_{imm}, and stops at the desired position. It is also an event from which two phases follow each other, a transient phase corresponding to the decelerating motion until the stop, noted ϕ_{fall}, and another one in which the robot configuration is maintained in a equilibrium position, ϕ_{stop}. To realize a more natural motion, the transient phases and the one of established motion should be customizable. Let ε_f be the duration of ϕ_{fall} and ε_r that of ϕ_{rise}. These settings depend on the nature of the manipulated object, its environment and the operator's capabilities. The customization of the transient part should allow adjusting the reaction time to match the minimum effort that can apply the operator, according to his abilities. The setting of the established motion phase should be compatible with the constraint imposed on the IP's velocity, i.e. with a velocity of constant and moderate amplitude, noted V_0. Only the duration control of ϕ_{stop} and ϕ_{cruise} is left to the HO's decision. Hence, the interaction force processing allows the identification of the initiation moment of the rising or the falling phase (denoted t_0), making thus the OTG event-controlled with two discrete states governed by the automaton of Figure 2. This moment is captured by comparing continuously the magnitude of this force with f_{th}. The sequencing of each phase always follows the same closed periodical cycle as depicted in Figure 2.

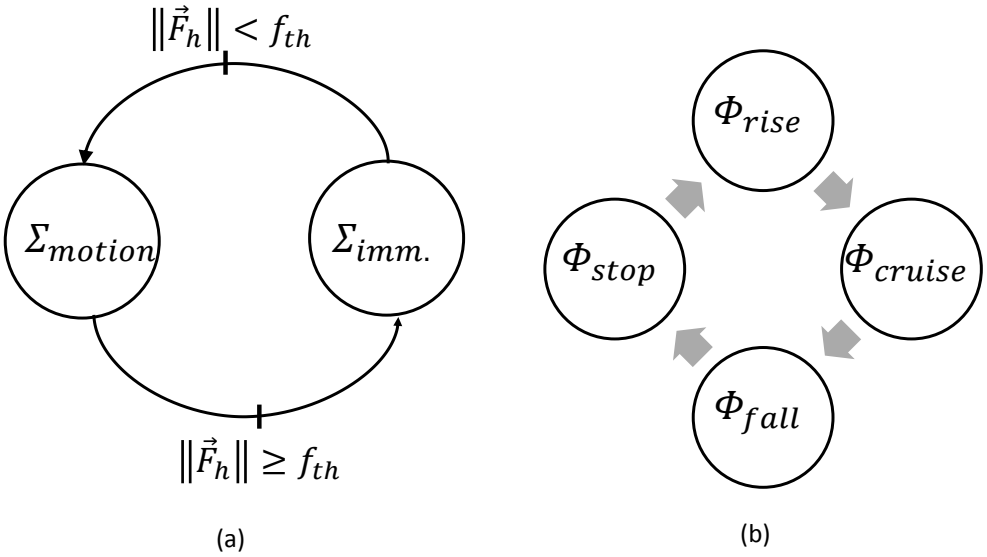

Figure 2: Automaton governing the motion states (left). Periodical cycle of phases (right).

b) Low-jerk velocity profile

The role of the OTG is to convert the real-time processing of the interaction force into displacement instructions of the IP, that depend on the phase in which is the HRI. These instructions should rely on a specific velocity profile, noted $V_p(t)$,

that meets the expected requirements on the norm of the desired velocity at the IP (noted $\dot{\overrightarrow{X}}_d$), viz safety, transparency and fluidity of movement interaction. A clear understanding of the human arm motions, as studied extensively by authors in (Tee et al., 2010), should contribute to a better consideration of the co-manipulation requirements in the definition of the trajectories to track. However, for simplicity and conciseness reasons of this paper, we made the choice of not including the human arm's dynamic to model the HRI in terms of force and common trajectories, whereas it should be included for a more rigorous and complete study. In return, a simpler representation of the HRI is considered. Since natural trajectories are required for a safe, smooth and comfortable interaction between the HO, the robot and the hanged load, we adopted the minimal-jerk trajectories to represent the HRI. Indeed, smoothness can be quantified as a function of jerk as reported in (Tamar Flash, 1985). It is now well established and experimentally demonstrated that limiting jerk is important for reducing the robot attrition as well as for improving fast and accurate tracking (Piazzi and Visioli, 2000). Moreover, it leads to a smoother control of the actuators, which reduces the excitation of the manipulator's fast dynamics such as vibrating modes. This consequently reduces danger for the HO, wear of the actuators, *etc*. To gather these specifications, the proposed low-jerk time function $V_p(t)$ imposed to $\left\|\dot{\overrightarrow{X}}_d\right\|$ and satisfying each phase's requirement is given by a piecewise defined polynomial based on the following quintic polynomial

$$V_p(t) = V_i + (V_f - V_i)\left(10\left(\frac{t-t_0}{T}\right)^3 - 15\left(\frac{t-t_0}{T}\right)^4 + 6\left(\frac{t-t_0}{T}\right)^5\right), \tag{6}$$

where T, V_i and V_f are parameters governed by the current HRI phase, as described in Table 1

Phase	Parameters setting	Velocity profile expression
ϕ_{stop}	$T \neq 0, V_i = 0, V_f = 0$	$V_p(t) = 0$
ϕ_{rise}	$T = \varepsilon_r, V_i = 0, V_f = V_0$	$V_p(t) = V_0\left(10\left(\frac{t-t_0}{\varepsilon_r}\right)^3 - 15\left(\frac{t-t_0}{\varepsilon_r}\right)^4 + 6\left(\frac{t-t_0}{\varepsilon_r}\right)^5\right)$
ϕ_{cruise}	$T \neq 0, V_i = 0, V_f = V_0$	$V_p(t) = V_0$
ϕ_{fall}	$T = \varepsilon_f, V_i = V_0, V_f = 0$	$V_p(t) = V_0\left(1 - 10\left(\frac{t-t_0}{\varepsilon_f}\right)^3 + 15\left(\frac{t-t_0}{\varepsilon_f}\right)^4 - 6\left(\frac{t-t_0}{\varepsilon_f}\right)^5\right)$

Table 1: Phase dependent velocity profile expression

c) Force direction processing

The desired velocity $\dot{\overrightarrow{X}}_d$ of the IP should remain collinear at every moment to the force exerted by the HO while having the same direction. Thus the angle formed by the IP's desired velocity and the interaction force $\left(\widehat{\dot{\overrightarrow{X}}_d, \overrightarrow{F}_h}\right)$ should be zero during the co-manipulation task, which is equivalent to ensuring $\dot{\overrightarrow{X}}_d \times \overrightarrow{F}_h = 0$ with $\left\langle \dot{\overrightarrow{X}} \,|\, \overrightarrow{F}_h \right\rangle > 0$. In other words, $\dot{\overrightarrow{X}}_d$ should have the same orientation angle than $\overrightarrow{F}_h$, namely θ_h. So, the direction to track, given by the unitary vector $\overrightarrow{U}_{\theta_h}$, has to be extracted from the measured force $\overrightarrow{F}_h$. The force sensor delivers the coordinates of $\overrightarrow{F}_h$ in the end-effector frame. A simple use of rotational transformations gives the corresponding coordinates in task space frame, $F_h = \begin{bmatrix} F_x & F_y \end{bmatrix}^T$. Then, the orientation angle is given by $\theta_h = tan^{-1}\left(\frac{F_y}{F_x}\right)$. In consequence, once the desired norm of $\dot{\overrightarrow{X}}_d$ computed as indicated in Paragraph b), the coordinates of $\dot{\overrightarrow{X}}_d$ in task-space frame are easily derived by the relation: $\dot{\overrightarrow{X}}_d = V_p \overrightarrow{U}_{\theta_h}$. The desired position $\overrightarrow{X}_d$ is obtained by a coordinate numerical integration of $\dot{\overrightarrow{X}}_d$, using for example an Euler explicit method, whereas the corresponding acceleration ($\ddot{\overrightarrow{X}}_d$) is deduced through basic numerical differentiation. All those vectors are used in an Inverse Kinematic Model component (IKM) (Spong and M., 1989) in order to compute the relevant variables needed in our control structure, such as joint positions, velocities and accelerations.

d) Recursive algorithm

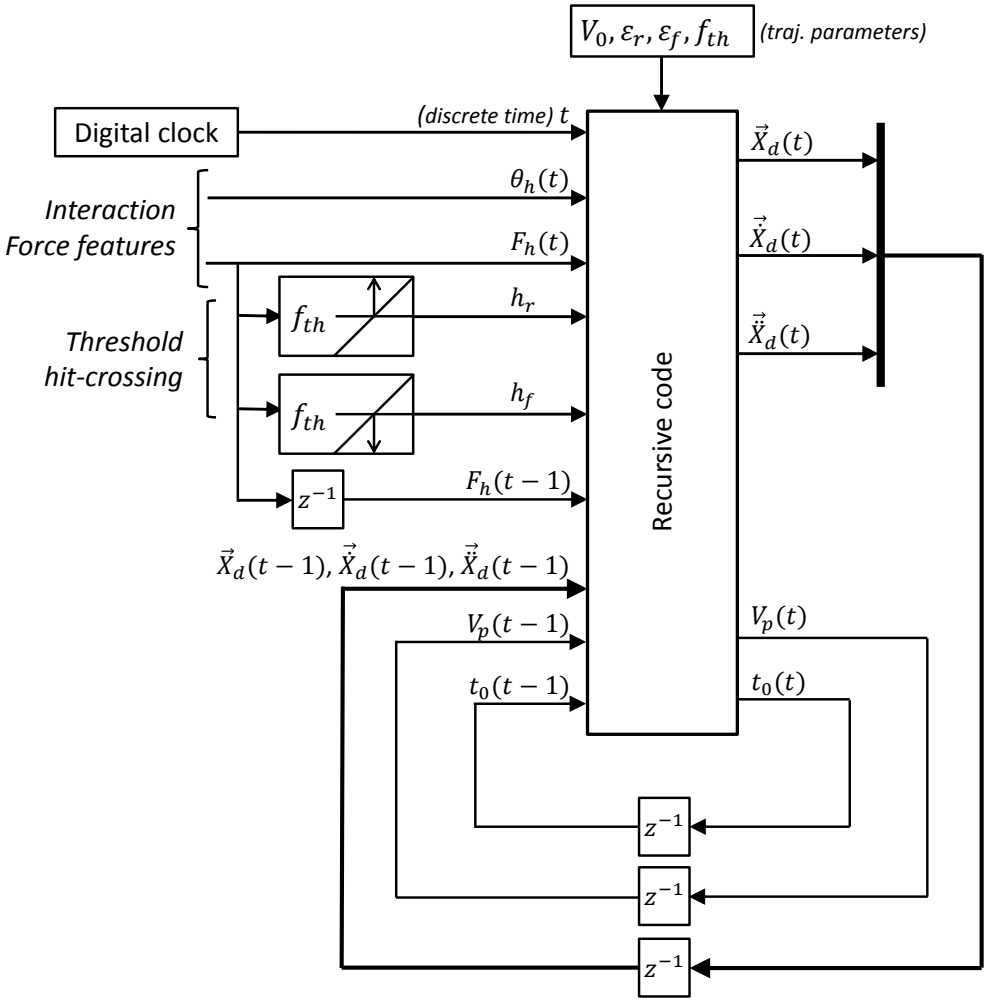

Figure 3: block-scheme of the recursive algorithm for generating the desired trajectory.

Because the human may change his desired motion unpredictably (a sudden presence of an obstacle, an unexpected change of destination *etc*), the real-time processing of the interaction force requires to store the starting and stopping moments of the robot's motion in memory cells, together with the values of the corresponding state i.e. position, velocity etc. Since the desired motion signals $\left(\vec{X}_d, \dot{\vec{X}}_d, \ddot{\vec{X}}_d\right)$ are generated in real-time, the information needed at the next computation cycle must be stored at each instant to allow. The algorithm for generation of these guidelines is necessarily recursive and can be represented by the block-scheme in Figure 3.

4.4 Impedance control

According to Tamar Flash (1985), the control objective of an impedance controller is to impose, along each direction of the task space, a desired dynamic relation between the manipulator end-effector position and the interaction force, the desired impedance. Usually, the desired impedance is chosen linear and of second order, as in a mass-spring-damper system. The end-effector velocity $\dot{X}$ and the interaction force F_h are related by a mechanical impedance function Z. In Laplace domain,

this is represented by:

$$F_h(s) = Z(s)\dot{X}(s). \tag{7}$$

In terms of position $X(s)$, we can write

$$F_h(s) = sZ(s)X(s), \tag{8}$$

where

$$sZ(s) = M_d s^2 + K_d s + K_p, \tag{9}$$

M_d, K_d and K_p are the desired inertia, damping and stiffness matrices of mass-spring-damper system respectively and s is the Laplace operator.

A knowledge of the geometric relation between coordinate frames is sufficient to transform any tensor from one frame to another. As in (Hogan, 1985), denote by $\mathscr{Y}(q)$ the inverse of the inertia matrix called the mobility tensor in joint coordinates. The kinematics transformations between joint space and task space coordinates define not only the relations between generalized displacements,flows and efforts in both coordinate frames but they also define the relation between the generalized momenta in joint and task space coordinates through the Jacobian. The mobility tensor expressed in task space $\mathscr{W}(q)$ is related to the mobility tensor in joint coordinates $\mathscr{Y}(q)$ as follows:

$$\mathscr{W}(q) = J(q)\mathscr{Y}(q)J^T(q). \tag{10}$$

Consider the control law

$$\tau = M(q)\hat{y} + C(q,\dot{q})\dot{q} + g(q) - J^T F_h, \tag{11}$$

where $\hat{y}$ represents a new input vector whose expression is to be determined. Substituting (11) in (1) we get:

$$M(q)\ddot{q} = M(q)\hat{y},$$

since the inertia matrix is invertible, we can write

$$\ddot{q} = \hat{y}.$$

According to (2) we have

$$\ddot{X} = J\hat{y} + \dot{J}\dot{q} \tag{12}$$

Let $\tilde{X} = X_d - X$, the operational space error between the desired and the actual end-effector position. The second order impedance control is as follow

$$M_d\ddot{\tilde{X}} + K_d\dot{\tilde{X}} + K_p\tilde{X} = JM^{-1}J^T F_h, \tag{13}$$

such as $JM^{-1}J^T$ is the mobility tensor. As in (Bruno Siciliano and Oriolo, 2009), the inertia M_d, damping K_d and stiffness K_p matrices are chosen to be constant diagonal positive definite. The expression of $\hat{y}$ is as follows

$$\hat{y} = J^{-1}M_d^{-1}\left(M_d\ddot{X}_d + K_d\dot{\tilde{X}} + K_p\tilde{X} - M_d\dot{J}\dot{q} - JM^{-1}J^T F_h\right). \tag{14}$$

5 Application and simulation results

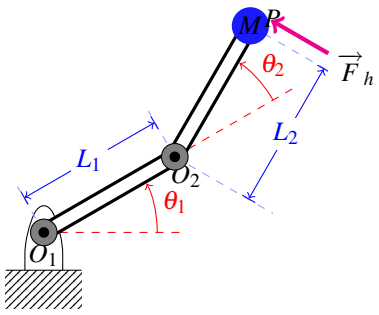

Figure 4: Two-link planar robot.

The current work focuses on illustrating the control strategy adopted through Two-link planar robot, depicted on Figure 4. Its architecture contains two revolute joints. The first one located at point O_1 where a motor exerts a control torque C_{m1}, and where θ_1 measures its position with respect to a fixed reference. The second is located at point O_2 where a motor exerts a control torque C_{m2}, and where θ_2 is defined as depicted in the picture. The end-effector is assumed to be at point P, where the human operator drives the robot and applies to it a force F_h that is measured. Let $J_\alpha = \left(\frac{m_1}{3} + m_2 + M\right) L_1^2$, $J_\beta = \left(\frac{m_2}{2} + M\right)$, $J_\gamma = \left(M + \frac{m_2}{3}\right) L_2^2$, $J_\varepsilon = \left(\frac{m_1}{2} + m_2 + M\right) L_1$ et $J_\eta = L_1 L_2$. Denote by $q := \begin{bmatrix} q_1 & q_2 \end{bmatrix}^T = \begin{bmatrix} \theta_1 & \theta_1 + \theta_2 \end{bmatrix}^T$, and let $X := \begin{bmatrix} x_1^T & x_2^T \end{bmatrix}^T = \begin{bmatrix} x_{11} & x_{12} & x_{21} & x_{22} \end{bmatrix}^T = \begin{bmatrix} q_1 & q_2 & \dot{q}_1 & \dot{q}_2 \end{bmatrix}^T$.

The details of the motion equations (1) are given, in this case, by

$$M(q) := \begin{bmatrix} J_\alpha & J_\beta J_\eta \cos(x_{12} - x_{11}) \\ J_\beta J_\eta \cos(x_{12} - x_{11}) & J_\gamma \end{bmatrix}, \tag{15}$$

$$C(q) := \begin{bmatrix} 0 & -J_\beta J_\eta \sin(x_{12} - x_{11}) x_{22} \\ J_\beta J_\eta \sin(x_{12} - x_{11}) x_{21} & 0 \end{bmatrix}, \tag{16}$$

$$g(q) := \begin{bmatrix} J_\varepsilon g \cos(x_{11}) \\ J_\beta L_2 g \cos(x_{12}) \end{bmatrix}. \tag{17}$$

The following simulations were done using `MATLAB` and `Simulink`. The parameters are $m_1 = 10\,[kg]$, $m_2 = 8\,[kg]$, $M = 2\,[kg]$, $L_1 = 5\,[m]$, $L_2 = 4\,[m]$ and $g = 9.81\,[m/s^2]$. The rise and fall times are set to $\varepsilon_r = \varepsilon_f = 0.3\,[s]$. The thresholds are as follows: $f_{th} = 1\,[N]$ and $f_{th-} = 0.75\,[N]$. As a first step, in order to emphasize the importance of the collinearity criterion, a *simulation test* was done. To move the robot from an initial position $q_1^i = -\pi/3$, $q_2^i = \pi/18$ to a final one $q_1^f = -\pi/6$, $q_2^f = \pi/4$, the HO needs to apply a force whose magnitude and direction are as shown in Figure 5 (left). One can easily see that the criterion of collinearity between force and velocity is not satisfied.

For the case of co-manipulation, we chose to model a human operator using a force having the same direction (orientation) than that of the *simulation test*, but with a considerably lower amplitude, in order to emphasize the satisfaction of assistance criterion *i.e.*the robot ensures the provision of the necessary power to move the handled object or to maintain it in the desired equilibrium position. the magnitude of the HO force, limited to maximum $3N$, is depicted in Figure 6 as well as the end-effector velocity profile. In this figure, we chose to increase the reaction time to $1s$ in order to distinguish the different succeeding motion states, depending on the position of F_h with respect to the force thresholds. *Stop* corresponds to the immobility phase with a null velocity, *Cruise* indicates no change in the velocity profile with a constant velocity. It corresponds to the phase of the established motion. *Ramp* designates the motion state change.

As described in Section 2, Ikeura et al. have shown that when dealing with a co-manipulation problem, the damping parameters in the impedance model are the predominant coefficients, they demonstrated experimentally that the effects of stiffness and inertia parameters are negligible. Thus, we set the impedance parameters as follows: $M_d = diag(1,1)$, $K_d = diag(198,198)$ and $K_p = O_{2,2}$. The trajectory tracking simulations for the obtained control law are depicted in Figure 7. We can see an excellent trajectory tracking for both position and velocity. Figure 8 highlights the fulfillment of the requirement of collinearity between the force applied by the HO and the velocity of the end-effector. This collinearity is obviously observed during the movement phase. When the norm of the applied force crosses the threshold f_{th} (dashed-brown), the velocity of the end-effector quickly follows the orientation of the force and it remains collinear till the moment when h_f switch to 1.

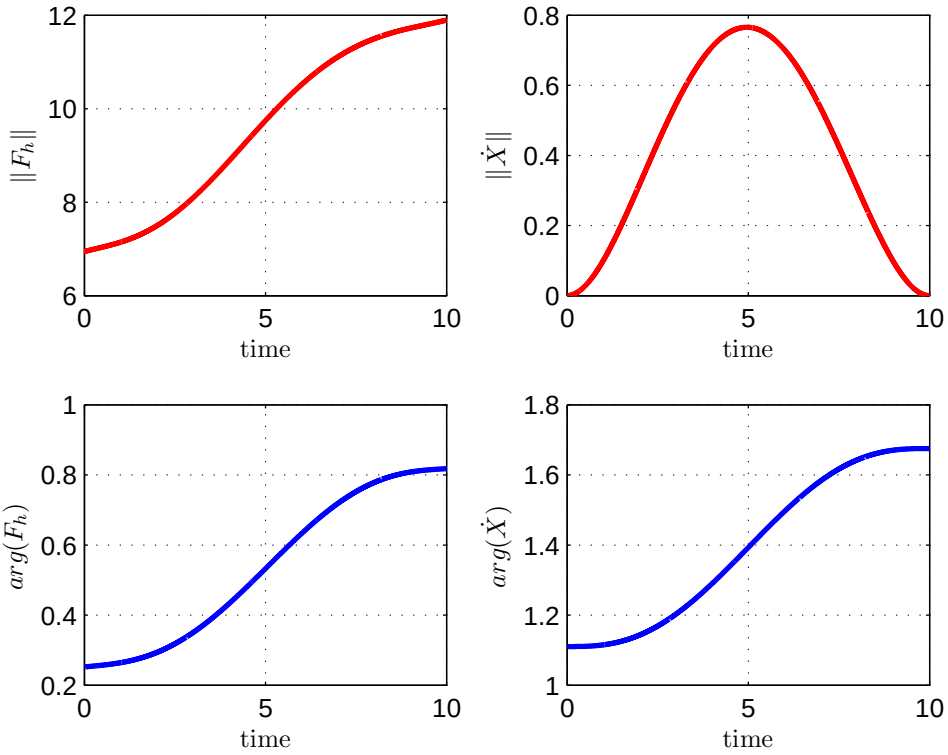

Figure 5: Force F_h versus end-effector velocity case of *simulation test*

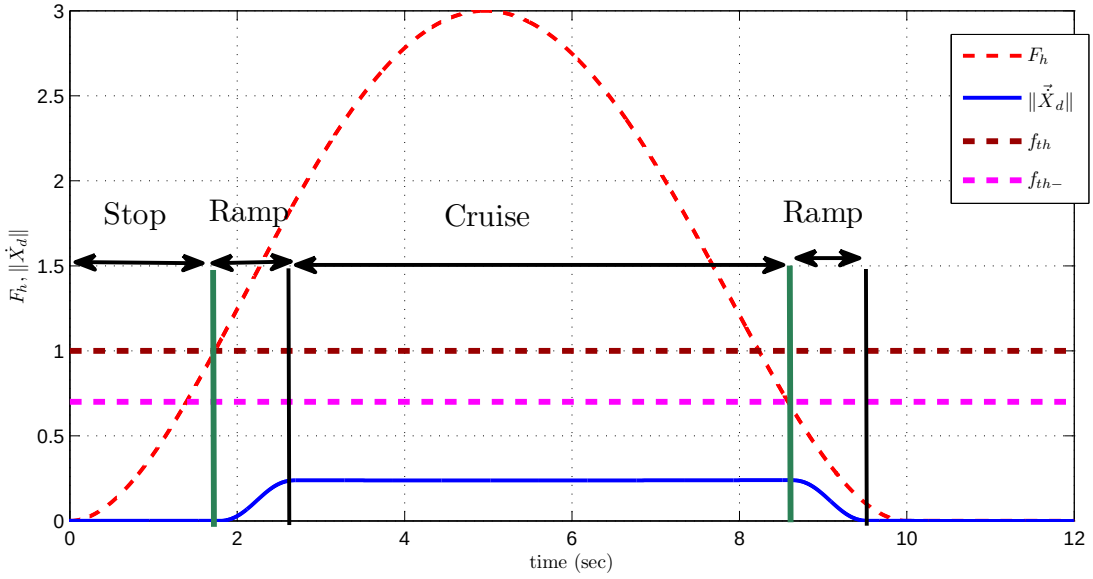

Figure 6: Desired velocity profile generated by processing the measurement of interaction force F_h.

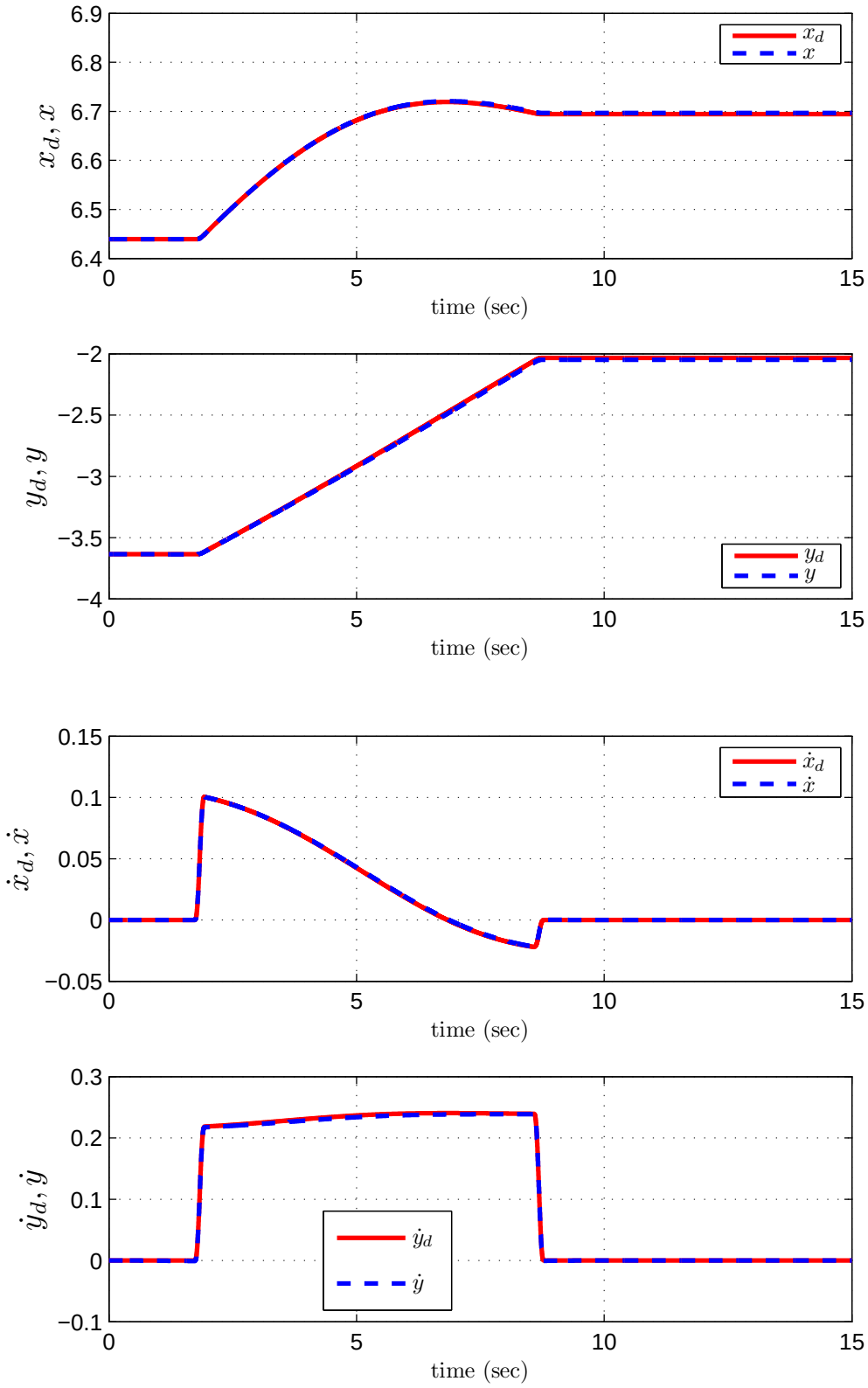

Figure 7: Position and velocity tracking.

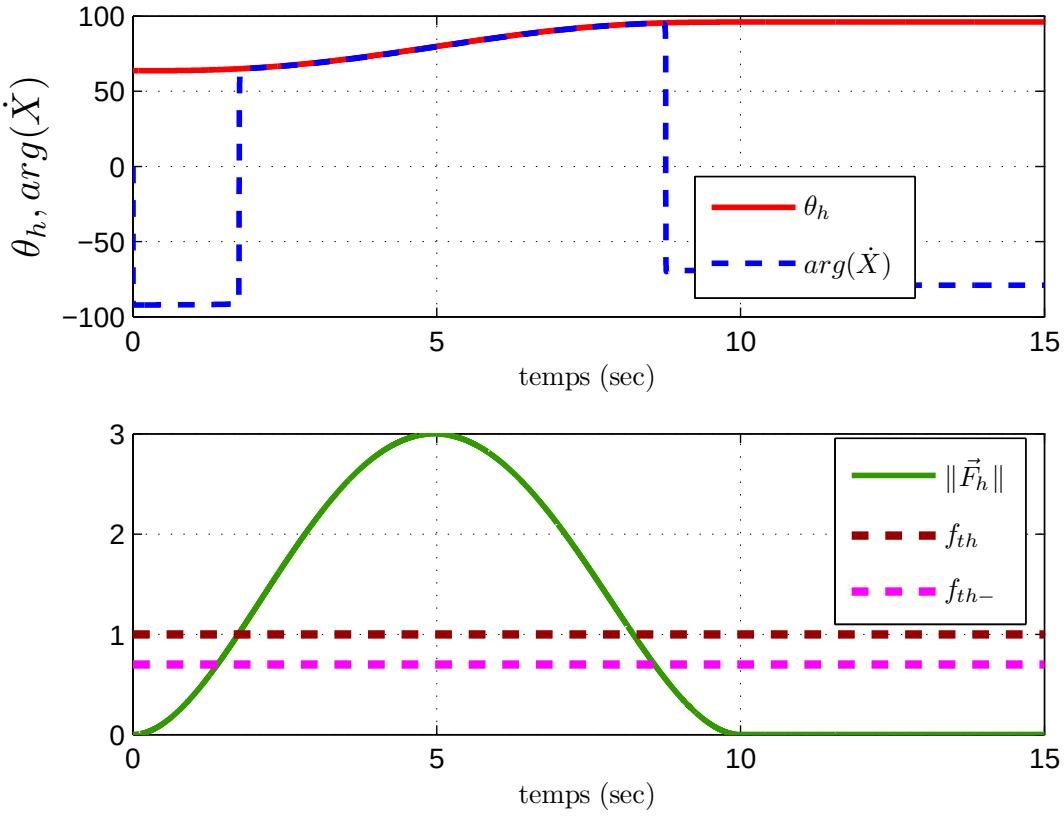

Figure 8: Collinearity between the HO applied force and the velocity of the end-effector.

6 Conclusion

This paper addressed the co-manipulation problem for handling tasks through a modified impedance control method named *Online Trajectory-Based Impedance (OTBI) Control*. This approach mainly lies on the implementation of a specific event-controlled online trajectory generator (OTG), that delivers trajectories to track when the operator exerts a force which amplitude is greater than a given threshold of low intensity, associated to a classical structure of impedance control insuring a very good tracking of the generated trajectory and maintaining the immobility of the robot configuration when there is no interaction force.

References

Akella, P., Peshkin, M., Colgate, E., Wannasuphoprasit, W., Nagesh, N., Wells, J., Holland, S., Pearson, T., and Peacock, B. (1999). Cobots for the automobile assembly line. In *Robotics and Automation, Proc. of 1999 IEEE Int. Conf. on*, volume 1, pages 728 –733 vol.1.

Bruno Siciliano, Lorenzo Sciavicco, L. V. and Oriolo, G. (2009). *Robotics: Modelling, Planning and Control*. Springer-Verlag.

Buerger, S. (2005). *Stable, High-force, Low-impedance Robotic Actuators for Human-interactive Machines*. Massachusetts Institute of Technology, Department of Mechanical Engineering.

Charnnarong, J., Hogan, N., Krebs, H. I., and Sharon, A. (1995). Interactive robot therapist. In *U.s.Patent*, volume 5.

Duchaine, V. and Gosselin, C. (2009). Safe, stable and intuitive control for physical human-robot interaction. In *Robotics and Automation, 2009. ICRA '09. IEEE International Conference on*, pages 3383–3388.

Hogan, N. (1985). Impedance control - An approach to manipulation. I - Theory. II - Implementation. III - Applications. *ASME Transactions Journal of Dynamic Systems and Measurement Control B*, 107:1–24.

Ikeura, R. and Inooka, H. (1995). Variable impedance control of a robot for cooperation with a human. In *Robotics and Automation, 1995. Proceedings., 1995 IEEE International Conference on*, volume 3, pages 3097–3102 vol.3.

Ikeura, R., Moriguchi, T., and Mizutani, K. (2002). Optimal variable impedance control for a robot and its application to lifting an object with a human. In *Robot and Human Interactive Communication, 2002. Proceedings. 11th IEEE International Workshop on*, pages 500–505.

Jlassi, S., Tliba, S., and Chitour, Y. (2012). On human-robot co-manipulation for handling tasks: Modeling and control strategy robot control. *10 th IFAC Symposium on robot control, SYROCO 2012, Dubrovnik, Croatie*, 10(710-715).

Kazerooni, H. and Guo, J. (1993). Human extenders. *Journal of Dynamic Systems, Measurement and Control*, 115:281 – 290.

Kroger, T. (2012). On-line trajectory generation: Nonconstant motion constraints. In *Robotics and Automation (ICRA), 2012 IEEE International Conference on*, pages 2048–2054.

Lamy, X., Colledani, F., Geffard, F., Measson, Y., and Morel, G. (2010). Human force amplification with industrial robot: Study of dynamic limitations. In *Intelligent Robots and Systems (IROS), 2010 IEEE/RSJ Int. Conf. on*, pages 2487 –2494.

Miyhoshi, T. and Murata, A. (2000). Chaotic characteristic in human hand movement. In *Robot and Human Interactive Communication*, pages 194 –199.

Moon, S. and Virk, G. (2009). Survey on iso standards for industrial and service robots. In *ICCAS-SICE, 2009*, pages 1878–1881.

Piazzi, A. and Visioli, A. (2000). Global minimum-jerk trajectory planning of robot manipulators. *Industrial Electronics, IEEE Transactions on*, 47(1):140–149.

Santis, A. D., Siciliano, B., Luca, A. D., and Bicchi, A. (2008). An atlas of physical human–robot interaction. *Mechanism and Machine Theory*, 43(3):253 – 270.

Spong, M. and M., V. (1989). *Robot dynamics and control*. John Wiley and Sons, Inc.

Surdilovic, D. (1996). Contact stability issues in position based impedance control: theory and experiments. In *Robotics and Automation, 1996. Proceedings., 1996 IEEE International Conference on*, volume 2, pages 1675–1680.

Tamar Flash, N. H. (1985). the coordination of arm movements an experimentally confirmed mathematical model. *The Journal of Neurosciences.*, 5(7):1688–1703.

Tee, K. P., Franklin, D. W., Kawato, M., Milner, T. E., and Burdet, E. (2010). Concurrent adaptation of force and impedance in the redundant muscle system. *Biol. Cybern.*, 102(1).

Tsumugiwa, T., Yokogawa, R., and Hara, K. (2002). Variable impedance control based on estimation of human arm stiffness for human-robot cooperative calligraphic task. In *Robotics and Automation, 2002. Proceedings. ICRA '02. IEEE International Conference on*, volume 1, pages 644–650 vol.1.